STM JOURNALS

International Journal of
Electrical Power and Machine Systems

Volume 3, Issue 2, 2025
July—December
DOI (Journal): 10.37591/IJEPMS

https://journals.stmjournals.com/ijepms

Review IJEPMS

Hardware Solution for LVRT Enhancement Techniques in DFIG: A Review

Sudeep Thapaliya[1,]*, A.H.M.A. Rahim[2]

Abstract

With the advancement of wind power technology, the penetration of wind power into power systems has increased significantly. Grid codes require that the wind generators remain connected for a specified time even under low-voltage conditions. Stricter grid code requirements are now necessary to ensure system stability and reliability due to the growing integration of wind power into contemporary power networks, which is being pushed by the quick development of wind energy technology. During low-voltage disruptions, these regulations compel wind turbines to stay connected to the grid for a predetermined amount of time. However, a doubly fed induction generator (DFIG) is extremely vulnerable to voltage drops since its stator is directly connected to the grid. Electrical failures, thermal loads, and extreme mechanical stress can all be brought on by prolonged or recurrent exposure to such conditions. Many protection and control strategies have been created to overcome these obstacles and allow for efficient low-voltage ride through (LVRT) functionality in DFIG-based wind energy systems. The stator of a DFIG is directly connected to the grid, which makes it very sensitive to the dips in grid voltage. Continuous operation of DFIG for multiple dips will lead to different mechanical and electrical system failures. Various protection schemes are proposed by researchers to ensure the continuous and healthy operation of DFIG riding through low voltage (LVRT) conditions. The most recent hardware-based LVRT augmentation methods put out in the literature are thoroughly reviewed in this work. The performance, cost, complexity, and dependability of various protection topologies and the control systems that go with them are all thoroughly examined and contrasted. To provide a comprehensive grasp of each approach's actual applicability, its advantages and disadvantages are emphasized. To help researchers and industry practitioners choose and create efficient hardware solutions for enhancing the LVRT capability and operational resilience of DFIG-based wind power systems, this paper attempts to be a useful resource.

Keywords: Doubly fed induction generator (DFIG), low-voltage ride through (LVRT), fault current limiter, DC-chopper, crowbar, Series dynamic braking system, energy storage

INTRODUCTION

Conventional energy sources are expensive and have limited availability. Additionally, fossil fuels are a source of pollution. This has led power industries to focus on green and clean energy sources. Currently, large investments are being made in the present to explore solar and wind energies. According to the International Energy Agency (IEA), wind energy plays a prominent role in reducing dependency on conventional energy sources [1, 2].

Owing to features such as reduced inverter cost, reduced cost of filters, and improved system efficiency, doubly fed induction generators (DFIG) are superior to other wind generators [3]. The stator of a DFIG is connected directly to the grid, whereas

***Author for Correspondence**
Sudeep Thapaliya
E-mail: thapaliyasudeep@gmail.com

[1]Assistant Professor, Department of Electrical and Electronic Engineering, United Technical College, Chitwan, Nepal
[2]Professor, Department of Electrical and Electronic Engineering, Brac University, Merul Badda, Dhaka, Bangladesh

Received Date: October 13, 2025
Accepted Date: October 14, 2025
Published Date: December 23, 2025

Citation: Sudeep Thapaliya, A.H.M.A. Rahim. Hardware Solution for LVRT Enhancement Techniques in DFIG - A Review. International Journal of Electrical Power and Machine Systems. 2025; 3(2): 59–73p.

the rotor is connected through back-to-back converters. The rotor frequency and voltage are varied using a rotor side converter (RSC) to maintain a constant output voltage and frequency [4, 5]. Low-voltage ride through (LVRT) capability is the ability of a DFIG to remain connected to the grid for a certain voltage dip for the specified time as per the grid code requirements. With advancements in technology, a large number of wind turbines have been connected to the grid. Owing to the large power penetration of the grid, it is not feasible to disconnect the DFIGs during fault conditions. Otherwise, there is a huge power imbalance in the system, and the entire network may collapse. Furthermore, the DFIG should supply a certain amount of reactive power to the system to fulfill the reactive power demand to support the grid voltage after fault clearance [6–8].

During a voltage dip, a natural flux producing a high-back electromagnetic force is induced on the rotor of the DFIG, which leads to an increase in the stator and rotor currents beyond the safe limit. Due to a high voltage sag, the grid side converter (GSC) will not be able to supply power to the grid. This causes an imbalance in the converter power, leading to an increase in the DC-link voltage and damaging the converters [9]. An imbalance between the mechanical and electrical torques may lead to mechanical failure owing to rotor overspeed. Various protection schemes have been proposed to ensure safe and continuous operation of DFIG in such cases [10]. Various hardware solutions presented in the literature to address some of these problems are briefly described below.

HARDWARE SOLUTION

The hardware solution focuses on the addition of extra physical equipment with a DFIG for LVRT improvement. The role of the hardware is to absorb surplus power, that is, an imbalance of mechanical and electrical power, according to the requirements of the grid system, as shown in Figure 1. Hardware solutions are typically combinations of resistors, inductors, and capacitors placed in different locations with unique orientations. The possible locations for the placement of these hardware devices, as proposed by different papers, are shown in Figure 1. The roles of these components differ according to their locations.

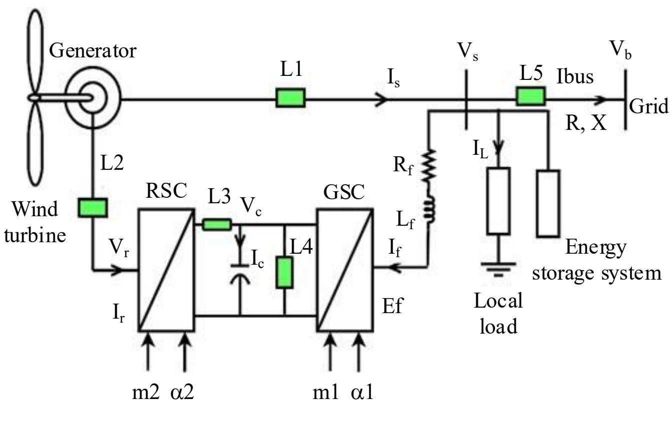

L1 = Stator side L2 -Rotor side L3 -Between RSC and capacitor

L4-Across DC-link capacitor L5=Grid side

Figure 1. Possible locations of different hardware for LVRT improvement.

CROWBAR

A crowbar is a commonly proposed hardware solution for LVRT improvement of the DFIG. The crowbar is installed on the rotor side between the rotor winding and the RSC converters [11, 12], as shown in Figure 1 (L2). The crowbar limits the rotor current with the insertion of external resistance. In this mode, the RSC is turned off, and the DFIG works as a conventional induction machine. DFIG absorbs reactive power from the power system to create a magnetic field. Because of the absorption of reactive power, the voltage dip will be worsened [13, 14]. To meet the reactive power requirements of the grid and DFIG, additional equipment is required, which adds to the cost. To overcome this problem, an optimized strategy for switching crowbars was proposed [15].

Improper switching and an inappropriate crowbar resistance value create an imbalance in the system. A high value of crowbar resistance leads to an increase in the DC-link voltage, whereas a low value may not be sufficient to control the transient fault current. In addition, if the crowbar activation time is short, the transient cannot be properly considered. If the activation time is high, the DFIG consumes more reactive power. The criteria for the selection of appropriate crowbar reactance values and switching times are provided [16, 17]. The authors concluded that an appropriate crowbar reactance value and switching time can improve LVRT for grid stability. However, frequent switching of the crowbar circuit during a voltage dip may have different impacts on the rotor circuit [18]. An adaptive crowbar resistor to support the dynamic reactive power was proposed [19].

SERIES DYNAMIC BRAKING RESISTOR

To overcome this drawback, the series dynamic braking resistor (SDBR) has been operating DFIG as an induction generator during crowbar activation. The SDBR placed on the rotor side, shown in Figure 1 (L2), does not require the RSC controller to turn off. In this case, the DFIG will be prevented from working as a conventional induction generator. The circuit diagram of the SDBR is shown in Figure 2.

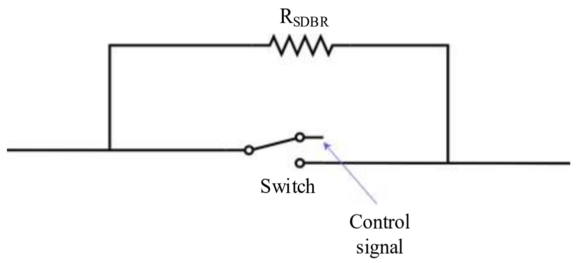

Figure 2. Configuration of SDBR.

During normal operation, the bypass switch is closed so that the current flows through a low-resistance path. During a fault on the grid, the bypass switch is opened, and the current flows through a high-resistance path. Energy was dissipated in the resistor. The SDBR helps to balance the active power and boost the generator voltage during a dip [20]. The resistance was chosen according to the temperature limit of the resistive element. In addition, the maximum heat dissipation capacity of the resistive element of the SDBR must be considered [21].

An single-bridge boost rectifier (SBBR) alone will lead to a high DC-link voltage, so it is suggested to use a hybrid model with the addition of a DC-chopper [22]. It is shown that the placement of the SDBR at the stator side (Figure 1; L1) instead of the rotor side (Figure 1; L2) provides optimal performance. Different techniques have been used to generate control signals for SDBR switching. During a fault, there is a change in the bus voltage, and the DFIG responds to signals such as rotor current, stator current, and DC-link voltage. Using the deviation of the grid voltage to generate the switching signal is more effective than using the deviation of the rotor current and DC-link voltage [23]. For less severe fault occurrences at instances of low wind speed, the low resistance of the SDBR is preferred. However, for more severe faults during high wind speeds, a higher resistance value of the SDBR yields better performance [24]. SDBR integration with a converter control scheme generally provides a better performance [25].

ENERGY STORAGE SYSTEM

If the energy lost during a low voltage can be stored, it can be returned after the clearance of the fault. One method to store energy is to use superconducting magnetic storage (SMES) systems. A magnetic energy storage device stores surplus power in the superconducting coil during a fault. Two major problems faced by DFIG are the low voltage and fluctuation of the output power owing to frequent changes in wind speed. The SMES system was proposed [26] to address both issues simultaneously. A superconducting coil (SC) has the dual job of balancing the output power during normal conditions and limiting the overcurrent during faults. Coordinated control of power converters along with transient reconfiguration to support LVRT with an energy storage device (ESD) has been suggested, where a demagnetizing current is used to counteract the negative-sequence stator current and reactive power supply simultaneously [27]. A novel configuration scheme is used where proper distribution of the rotor current component between the RSC and energy storage converters (ESC) is carried out to optimize the capacity of the ESD [28]. The energy storage device-unified power quality conditioner (ESD-UPQC) contributes to improving the LVRT capability, regulating the output power, and limiting voltage oscillations [29]. The cooperative control of rotor side SMES and transient control [30], coordination of the active crowbar along with the battery energy storage system (BESS) [31], and flywheel as an energy storage system [32] are other techniques described in the literature for LVRT enhancement. The BESS contributes to bringing the system back to a stable state after disturbance [33, 34]. A series-connected current source converter (CSC)-based SMES is simple in structure and easy to control for LVRT enhancement [35].

DC-LINK CHOPPER

A DC-link chopper was used as the protection scheme to maintain the DC-link voltage during low-grid-voltage conditions. During a dip, the converter will not be able to inject power in the full range to the output terminal because of a decrease in the terminal voltage, which leads to an increase in the DC-link voltage. If the DC-link voltage is high beyond this limit, it may damage the converters. To overcome this problem, choppers are being used to protect the converters and ensure the smooth functioning of the DFIG during disturbance. The chopper was placed in parallel between the DC-link capacitors (Figure 1; L4). The DC voltage was compared with a certain reference value, and the control signal was generated, as shown in Figure 3 [36, 37].

The DC-chopper was implemented in a DFIG integrated power system to observe its effectiveness. The experimental results show that the DC-chopper performance is better than that of a crowbar [38]. The power absorbed by the chopper resistance during its activation is expressed as

$$P_{absorbed} = \frac{V_{dc}^2}{R_{chopper}} \tag{1}$$

Where, $P_{absorbed}$ is the active power absorbed by the chopper, V_{dc} is the DC-link voltage, and $R_{chopper}$ is the chopper resistance. Simulation results verified that the system performance is not as good for large values of the chopper resistance [39]. It is suggested that quicker insertion and operation for a short duration yields better results. A comparative analysis of a hybrid system, that is, supplementary rotor current control in the RSC with chopper and SDBR, was conducted [40]. It is observed that the chopper with the SDBR provides better system performance despite being slightly more expensive. A DC-chopper was integrated with a multi-terminal high voltage direct current (HVDC) in an offshore wind farm for LVRT enhancement [41].

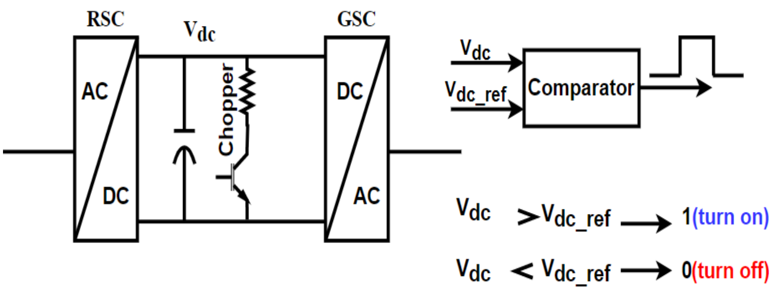

Figure 3. DC-chopper configuration with controller.

A modified DC-chopper replacing the conventional chopper was proposed [42], as shown in Figure 4. This study uses differential control logic for switching so that it can operate as a chopper as well as a fault current limiter according to the system demand. An AI-based chopper crowbar protection scheme was proposed [43]. An adaptive neuro-fuzzy inference system (ANFIS) is used in the proposed model to detect faults in the system and generate control signals for hardware activation. The rotor side superconducting fault current limiter (SFCL) (Figure 1; L2) with a DC-link brake chopper can successfully maintain grid stability during disturbances [44]. The stator-side SFCL (Figure 1; L1) with a DC-link chopper was proposed [45] for high voltage ride through (HVRT) improvement. The choppers function as the primary protection to limit the DC-link voltage. The SFCL contributes to electromagnetic torque and overcurrent protection.

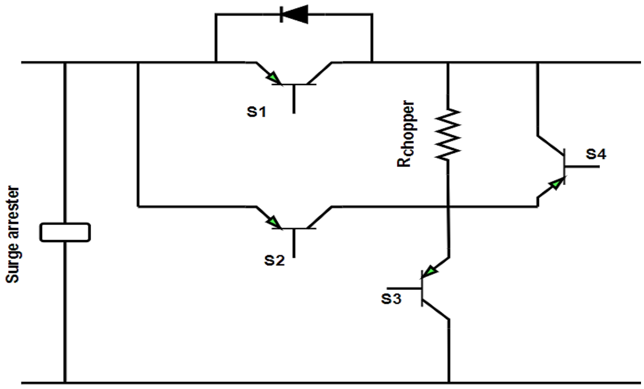

Figure 4. Modified DC-chopper configuration.

SUPERCONDUCTING FAULT CURRENT LIMITER

An SFCL is electrical equipment that possesses negligible resistance during normal operating conditions and provides high resistance during a fault. If any of the parameters, such as temperature, current density, and magnetic field, rise above the critical values, the resistance will increase exponentially, limiting the fault current. The major advantages of SFCL over other hardware solutions are its self-quenching and self-healing properties. In protection schemes involving mechanical switching and control, there is a probability that the switch will fail. Such a problem can be addressed with the use of the SFCL, as it does not require any control action to change its state [46]. The various types of SFCL proposed in the literature are as follows.

Resistive SFCL

The resistive SFCL is connected in series with the power system network. The equivalent model of the resistive SFCL is given as [47, 48]:

$$R(t) = \begin{cases} 0 & t < t_0 \\ R_m\left[1 - exp\left(-\frac{t-t_0}{T_f}\right)\right] & t_0 \le t < t_1 \\ a_1(t-t_1) + b_1 & t_1 \le t < t_2 \\ a_2(t-t_2) + b_2 & t_2 \le t < t_3 \end{cases} \quad (2)$$

Here, R(t) is the SFCL resistance at different states, R_m is the maximum resistance in the quenching state, T_f is the time constant, t_0 is the time to start quenching, t_1 is the 1st recovery time, t_2 is the 2nd recovery time, t_3 is the complete recovery time, and a_1, a_2, b_1 and b_2 are the functional coefficients. The quenching and recovery time characteristics are shown in Figure 5.

A resistive SFCL placed at the rotor side (Figure 1; L2) of the DFIG was proposed [49]. The results obtained show that the implemented strategy succeeds in limiting the DC-link voltage, peak value of the rotor current, and electromagnetic torque to a safe limit during symmetrical and unsymmetrical faults. The detailed structural and conceptual design of the SFCL with a refrigeration system for cooling purposes [50]. The resistive SFCL is advantageous for its various features, such as rapid response, automatic trigger, and excellent current limiting ability [51].

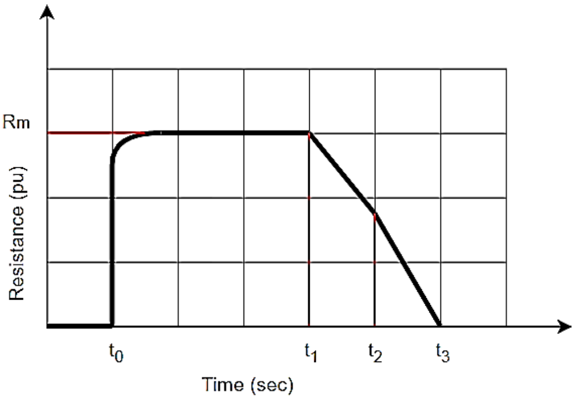

Figure 5. Quenching and recovery characteristics of resistive SFCL.

Inductive SFCL

To improve the LVRT capability of DFIG, an inductive SFCL was proposed [52]. The system configuration is shown in Figure 6 (Figure 1; L2). Under normal conditions, the developed structure acts as a filter. When a fault occurs, the combination of the SFCL with demagnetization technology limits the rotor overcurrent, ensuring safe operation of the DFIG. A comparative analysis of the impact of resistive and inductive SFCL is presented [53]. It is observed that both systems succeed in limiting the fault current and maintaining the DC-link voltage along with the electromagnetic torque; however, the resistive SFCL is superior in terms of the current limiting ratio and restraining capacity.

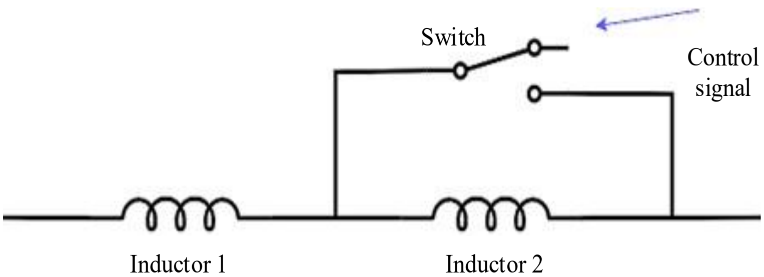

Figure 6. Inductive SFCL configuration.

DC-Resistive SFCL

A DC-resistive SFCL is a combination of a rectifier bridge and a resistive type SFCL, as shown in Figure 7 (Figure 1; L5). With the use of the bridge network, the AC loss in the superconductor is minimized, improving the system performance compared with that of the resistive SFCL. Owing to the self-quenching nature of the SFCL, no extra controller is required to trigger the R-SFCL during a

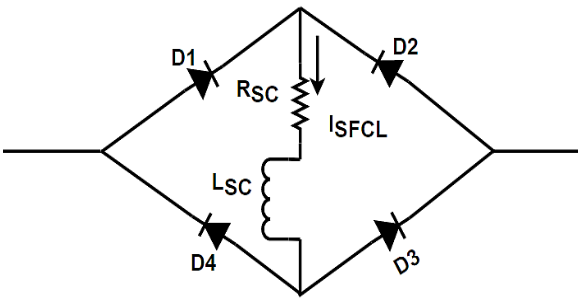

Figure 7. DC-resistive SFCL configuration.

fault [54]. During one half-cycle, the current flowed through D1-R_{sc}-L_{sc}-D3. The path for the other half-cycle is D2-R_{sc}-L_{sc}-D4; therefore, the current flowing through the SC is unidirectional. This scheme is the same for the other bridge networks, as described later.

Capacitive Bridge Type SFCL

The capacitive bridge type SFCL (CB-SFCL) given in Figure 8 (Figure 1; L5) is proposed [55]. In this scheme, a high-temperature superconductor (HTS) coil is maintained in series with a power capacitor. Here, the capacitor is activated through a controller only during a fault in the system. The addition of a capacitor makes it superior in operation compared to the DC-resistive SFCL, as it supplies adequate reactive power demand and also provides capacitive compensation while maintaining the terminal voltage of the DFIG in the safe range. The role of the metal-oxide varistor (MOV) in the CB-SFCL is to reduce the surge overvoltage caused by insulated gate bipolar transistor (IGBT) switching.

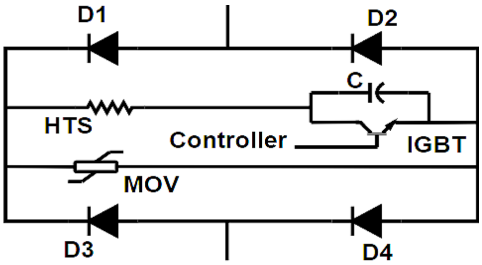

Figure 8. CB-SFCL configuration.

Modified Bridge Resistive SFCL

The configuration of the modified bridge resistive type SFCL (MBR-SFCL) is shown in Figure 9 (Figure 1; L5) [56]. It consists of a bridge, an IGBT switch for control, and a resistive SFCL. During normal operation, the IGBT is kept off, and the SFCL is in the superconducting state. During the fault current rise, R_{sc} increased to the peak value, limiting the current. The resistance of the MBR-SFCL was controlled by the duty cycle of the parallel IGBT. The expression for resistance is as follows:

$$R_{MBR-SFCL} = (1 - D) * R_{sc} \quad (3)$$

Where, D is the duty cycle of the IGBT, and R_{sc} is the SFCL resistance. Through controlled resistance, better performance is obtained compared with that of a conventional SFCL [57].

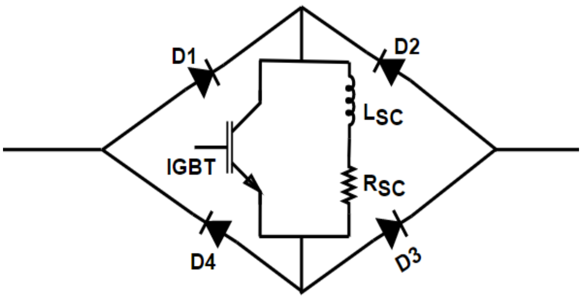

Figure 9. MBR-SFCL configuration.

Flux-Coupling SFCL

A modified flux-coupling-type SFCL was proposed [58]. The designed architecture of the SFCL is illustrated in Figure 10. During normal operation, the current flowing through the two windings is the same; therefore, the two inductors oppose each other. During the fault, S1 opens. The flux between the two windings does not cancel, and the SC is quenched to a higher resistance, limiting the overcurrent. The proposed scheme is analyzed by placing it in the stator (Figure 1; L1) and between the RSC and the DC-link capacitor (Figure 1; L3). This observation shows that when the SFCL is placed on the stator side, the terminal voltage sag can be improved.

A comparative analysis of the hybrid SFCL with a bias magnetic field (HSFCL) with SDBR and bridge-type fault current limiter (BFCL) was carried out. It is shown that the HSFCL performs better than the SDBR and BFCL. In addition, the response time of the HSFCL is much better, and it is more efficient [59]. A feedback non-linear control technique for controlling a flux-coupling-type SFCL has been proposed and demonstrated to be superior to the conventionally controlled flux-coupling SFCL [60, 61]. The conceptual design of the flux-coupling SFCL was carried out, and its performance was analyzed [62].

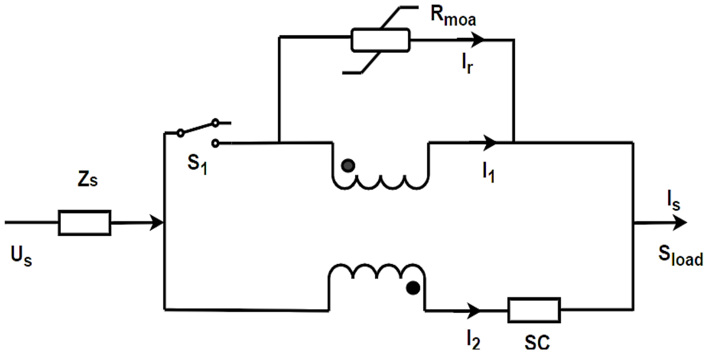

Figure 10. Flux-coupling SFCL configuration.

An active SFCL with voltage compensation was proposed [63]. Active SFCL have higher controllability and flexibility than resistive and inductive SFCL do. It was concluded that the active SFCL can strengthen the power system stability by smoothing the power fluctuation of the DFIG. The SFCL, along with RSC control, was proposed [64]. With the proposed scheme, the terminal voltage is maintained sufficiently to fulfill the grid code requirements. Cooperative control of the SFCL along with the SMES [65] and reactive power [66] is used to limit the overcurrent, and excess power is passed to the SMES to balance the power in the system while maintaining stability. Cooperative control provides superior control and reduces the SMES capacity, thereby making the overall system economical.

NON-SUPERCONDUCTING FCL (NSFCL)

The various types of NSFCL described in the literature are as follows.

Bridge Type FCL

BFCL with a shunt and a bridge is proposed [67], as shown in Figure 11, installed on the grid side (Figure 1; L5). The bridge part consists of diodes in a bridge configuration along with a DC reactor R_{dc}. An IGBT switch was used to control the bridge operation. During normal operation, the IGBT is ON; therefore, the current flows through a low-resistance path. During a fault, the IGBT is off, and the current is forced through the shunt path, thus limiting the current [68]. The freewheeling diode (D5)

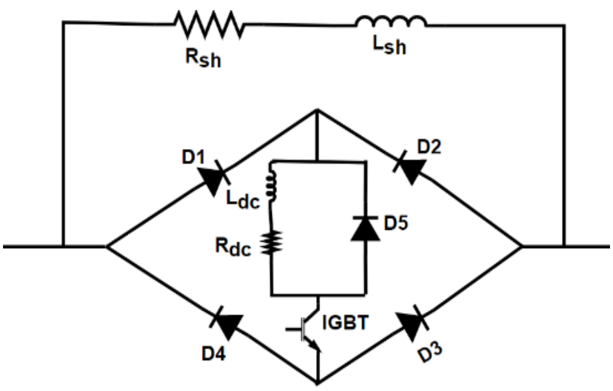

Figure 11. BFCL configuration.

discharged the residual current and protected the IGBT switch from overcurrent destruction. BFCL is superior in performance to the SDBR, but the SDBR is more economical. The control circuit for the generation of IGBT pulses was described in detail [69].

Capacitive Bridge Type FCL (CB-FCL)

With the insertion of an AC reactor in series during a fault in the BFCL, reactive power was absorbed from the grid. To overcome this problem, the inductor was replaced with a capacitor. In this scheme, reactive power is supplied to the grid, which supports the grid voltage during and after a fault [70]. The Fuzzy logic controller-based CB-FCL is capable of operating under different operating conditions [71]. The proposed scheme shown in Figure 12 was placed on the grid side (Figure 1; L5).

Nonlinear Controlled Modified Bridge-Type Fault Current Limiter (NC-MBFCL)

The modified BFCL consists of a resistor parallel to the bridge, as shown in Figure 13 (Figure 1; L5). Using a non-linear control system, a variable value of the effective shunt impedance is applied to the system instead of applying the full impedance value throughout the fault period. This observation shows that NC-MBFCL is very efficient for LVRT capacity enhancement of DFIG. It outperformed the conventionally controlled MBFCL and BFCL [72].

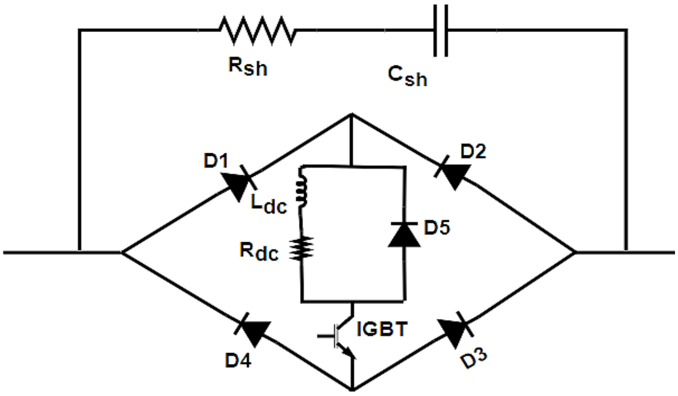

Figure 12. CB-FCL configuration.

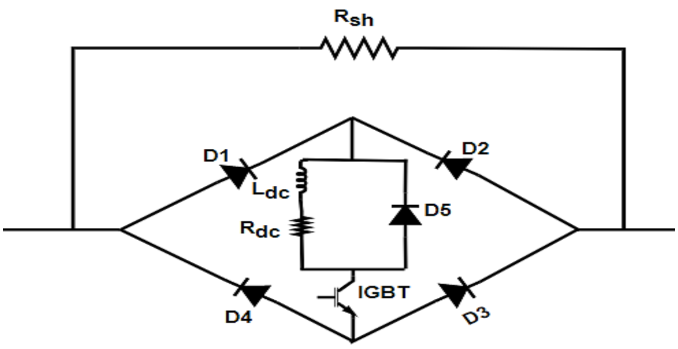

Figure 13. NC-MBFCL configuration.

Parallel Resonance BFCL (PRFCL)

In this scheme, the bridge of the PRFCL is the same as that of the BFCL. The shunt resonance path consists of a capacitor C_{sh} and an inductor L_{sh} placed in parallel, as shown in Figure 14. This network forms an inductor–capacitor (LC) resonance circuit at the power-line frequency [73]. During the fault, the IGBT switch opens and current flows through a high-impedance resonating shunt path. The proposed scheme is located on the grid side (Figure 1; L5). It was observed that PRFCL is effective in improving the LVRT capacity and maintaining the mechanical torque balance in a turbine generator system [74]. The performance of the hybrid system (DFIG, PV, and SG) PRFCL performance is compared with that of BFCL. The graphical plot, along with the index value, shows that PRFCL is superior [75]. Fuzzy logic control (FLC) is used to produce a duty cycle that controls the switching of the IGBT. With a change in the duty cycle, the shunt impedance can vary, which provides flexibility to the FLC-PRFCL to work efficiently for both symmetrical and unsymmetrical faults. Comparative analysis shows that FLC-PRFCL outperforms crowbar, BFCL, and conventional PI-PRFCL in terms of overall performance [76].

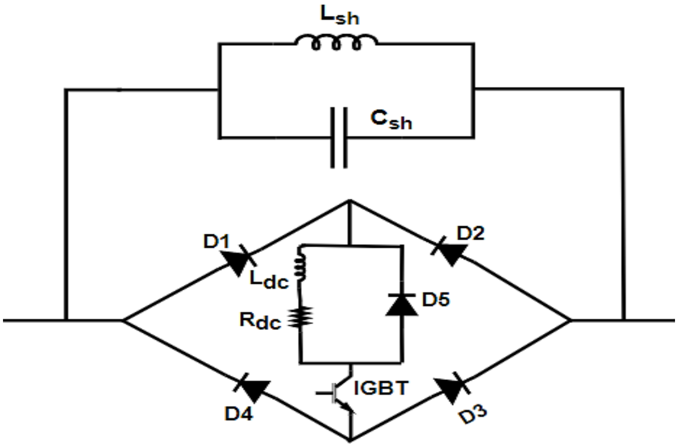

Figure 14. PRFCL configuration.

Neuro-fuzzy logic controller-based PRFCL (NFLC-PRFCL) is compared with fuzzy-based PRFCL (FLC-PRFCL) [77]. Simulation results show that NFLC-PRFCL provides 97.10% improvement in the Point of Common Coupling (PCC) voltage, whereas FLC-PRFCL provides 94.45% improvement.

CONCLUSION

A review of various hardware solution approaches for LVRT capability enhancement of the DFIG was carried out. The working principles and configurations of various techniques have also been studied. A crowbar is a simple conventional trend in solutions, but it has the disadvantage of consuming reactive power. A SDBR can limit the rotor and stator currents; however, the DC-link voltage is not considered. An energy storage system is an alternative approach; however, it is not economical to implement large systems. The DC-link chopper works best in limiting the DC-link voltage. Different approaches have been adopted to combine two or more solutions to render the overall system feasible and economical. Artificial intelligence is also integrated into a control system so that the control signal can be generated more precisely and accurately.

Some researchers have proposed the implementation of various superconducting and non-superconducting FCLs. The SFCL requires no control switch owing to its self-quenching property, which is advantageous; however, superconductors are costly, and the cooling system is complicated to implement. Different linear and non-linear control strategies are currently being tested for the optimization of FCL these days. Optimally operated SFCLs are currently among the best solutions.

Acknowledgements

The authors acknowledge the support provided by Brac University, Dhaka, and United Technical College, Nepal, for this work.

REFERENCES

1. Agarwal T, Verma S, Gaurh A. Issues and challenges of wind energy. 2016 International Conference on Electrical, Electronics, and Optimization Techniques (ICEEOT), Chennai, India. 2016. p. 67–72. doi:10.1109/ICEEOT.2016.7754761.
2. Sahoo SS, Roy A, Chatterjee K. Fault ride-through enhancement of wind energy conversion system adopting a mechanical controller. 2016 National Power Systems Conference (NPSC), Bhubaneswar, India. 2016. p. 1–5. doi:10.1109/NPSC.2016.7858936.

3. Müller S, Deicke M, De Doncker RW. Doubly fed induction generator systems for wind turbines: a viable alternative to adjust speed over a wide range at minimal cost. IEEE Ind Appl Mag. 2002;8(3):26–33. doi:10.1109/2943.999610.
4. El-Jalyly A, Derri M, Haidi T, Janyene A. Modeling and control of a DFIG for wind turbine conversion system using back-to-back PWM converters. 2019 7th International Renewable and Sustainable Energy Conference (IRSEC), Agadir, Morocco. 2019. p. 1–6. doi:10.1109/IRSEC48032.2019.9078332.
5. Arbi J, Ghorbal MJB, Slama-Belkhodja I, Charaabi L. Direct virtual torque control for doubly fed induction generator grid connection. IEEE Trans Ind Electron. 2009;56(10):4163–73. doi:10.1109/TIE.2009.2021590.
6. Duong MQ, Sava GN. Coordinated reactive power control of DFIG to improve LVRT characteristics of FSIG in wind turbine generation. 2017 International Conference on Electromechanical and Power Systems (SIELMEN), Iasi, Romania. 2017. p. 256–60. doi:10.1109/SIELMEN.2017.8123328.
7. Yan L, Yongning C, Zhen W, Linjun W, Chao L. Study on LVRT capability of D-PMSG based wind turbine. In: Proc IEEE Power Engineering and Automation Conf; 2011. Vol 1. Piscataway (NJ): IEEE; 2011.
8. Shin H, Jung HS, Sul SK. Low voltage ride-through control strategy of grid-connected variable speed wind turbine generator system. 8th International Conference on Power Electronics - ECCE Asia, Jeju, Korea (South). 2011. p. 96–101. doi:10.1109/ICPE.2011.5944552.
9. Rauth SS, Kastha D, Bajpai P. Comparative analysis of external configuration-based DFIG-LVRT enhancement schemes. 2020 21st National Power Systems Conference (NPSC), Gandhinagar, India. 2020. p. 1–6. doi:10.1109/NPSC49263.2020.9331951.
10. Vikas, Sahoo SS, Tripathi PM, Chatterjee K. A coordinated control strategy using rotor current limiter and switchable type series passive resistive fault current limiter for enhanced fault ride-through. 2017 7th International Conference on Power Systems (ICPS); 2017 Dec 21–23; Pune, India. 2017. p. 346–351. doi:10.1109/ICPES.2017.8387318.
11. Yang S, Zhou T, Zhen X, Zhang X, Shao R, Chang L. A SCR crowbar commutated with rotor-side converter for doubly fed wind turbines. 2015 IEEE 6th International Symposium on Power Electronics for Distributed Generation Systems (PEDG), Aachen, Germany. 2015. p. 1–7. doi:10.1109/PEDG.2015.7223084.
12. Li-Ling S, Pu Y, Yi W. Simulation research for LVRT of DFIG based on rotor active crowbar protection. International Conference on Sustainable Power Generation and Supply (SUPERGEN 2012). Stevenage (UK): Institution of Engineering and Technology; 2012. p. 107. doi:10.1049/cp.2012.1810.
13. Meegahapola LG, Littler T, Flynn D. Decoupled-DFIG fault ride-through strategy for enhanced stability performance during grid faults. IEEE Trans Sustain Energy. 2010;1(3):152–62. doi:10.1109/TSTE.2010.2058133.
14. Yang L, Xu Z, Østergaard J, Dong ZY, Wong KP. Advanced control strategy of DFIG wind turbines for power system fault ride-through. IEEE Trans Power Syst. 2012;27(2):713–22. doi:10.1109/TPWRS.2011.2174387.
15. Han J, Jia W, Wang Y, Zhou L, Hu H, Ren Y. An optimized strategy of switching crowbar improve LVRT of DFIG based on RTDS. 2020 IEEE Sustainable Power and Energy Conference (iSPEC), Chengdu, China. 2020. p. 775–80. doi:10.1109/iSPEC50848.2020.9351162.
16. Shi L, Chen N, Lu Q. Dynamic characteristic analysis of doubly-fed induction generator low voltage ride-through. Energy Procedia. 2012;16:1526–34. doi:10.1016/j.egypro.2012.01.239.
17. Renxiao WA, Huihui SO, Li HA, Luocheng YA, Bin WA, Pu ZH. Study on LVRT of DFIG wind power system based on crowbar protection circuit. 2018 IEEE Student Conference on Electric Machines and Systems, Huzhou, China. 2018. p. 1–6. doi: 10.1109/SCEMS.2018.8624855.
18. Li J, Qiu Q, Zhan M. An improved crowbar control circuit of DFIG during LVRT. 2021 IEEE 4th International Electrical and Energy Conference (CIEEC), Wuhan, China. 2021. p. 1–6. doi: 10.1109/CIEEC50170.2021.9510598.

19. He C, Tan Q, Zhang N, Chen J, Shen R, Wu X. Research on low voltage ride-through capability of DFIG based on adaptive crowbar resistor. 2018 37th Chinese Control Conference (CCC), Wuhan, China. 2018. p. 8930–8935. doi:10.23919/ChiCC.2018.8482616.
20. Okedu KE, Muyeen SM, Takahashi R, Tamura J. Application of SDBR with DFIG to augment wind farm fault ride-through. 2011 International Conference on Electrical Machines and Systems, Beijing, China. 2011. p. 1–6. doi:10.1109/ICEMS.2011.6073472.
21. Causebrook A, Atkinson DJ, Jack AG. Fault ride-through of large wind farms using series dynamic braking resistors. IEEE Trans Power Syst. 2007;22(3):966–75. doi:10.1109/TPWRS.2007.901658.
22. Soliman H, Wang H, Zhou D, Blaabjerg F, Marie MI. Sizing of the series dynamic braking resistor in a doubly fed induction generator wind turbine. 2014 IEEE Energy Conversion Congress and Exposition (ECCE), Pittsburgh, PA, USA. 2014. p. 1842–1846. doi:10.1109/ECCE.2014.6953642.
23. Okedu KE. Optimal position and best switching signal of SDBR in DFIG wind turbine low voltage ride-through capability. 2017 IEEE International Electric Machines and Drives Conference (IEMDC), Miami, FL, USA. 2017. p. 1–6. doi:10.1109/IEMDC.2017.8001868.
24. Huang J, Zhang L, Sang S, Xue X, Zhang X, Sun T, et al. Optimized series dynamic braking resistor for LVRT of doubly-fed induction generator with uncertain fault scenarios. IEEE Access. 2022;10:22533–46. doi:10.1109/ACCESS.2022.3154042.
25. Gatavi E, Hellany A, Nagrial M, Rizk J. Improved low voltage ride-through capability of DFIG-based wind turbine with braking resistor and converter control. 2018 IEEE 12th International Conference on Compatibility, Power Electronics and Power Engineering (CPE-POWERENG 2018), Doha, Qatar. 2018. p. 1–6. doi:10.1109/CPE.2018.8372517.
26. Guo W, Xiao L, Dai S. Enhancing low-voltage ride-through capability and smoothing output power of DFIG with a superconducting fault-current limiter–magnetic energy storage system. IEEE Trans Energy Convers. 2012;27(2):277–95. doi:10.1109/TEC.2012.2187654.
27. Shen YW, Ke DP, Qiao W, Sun YZ, Kirschen DS, Wei C. Transient reconfiguration and coordinated control for power converters to enhance the LVRT of a DFIG wind turbine with an energy storage device. IEEE Trans Energy Convers. 2015;30(4):1679–90. doi:10.1109/TEC.2015.2449900.
28. Shen YW, Ke DP, Sun YZ, Kirschen DS, Qiao W, Deng XT. Advanced auxiliary control of an energy storage device for transient voltage support of a doubly fed induction generator. IEEE Trans Sustain Energy. 2016;7(1):63–76. doi:10.1109/TSTE.2015.2472299.
29. Yang RH, Jin JX. Unified power quality conditioner with advanced dual control for performance improvement of DFIG-based wind farm. IEEE Trans Sustain Energy. 2021;12:116–26. doi:10.1109/TSTE.2020.2985161.
30. Xiao XY, Yang RH, Zheng ZX, Wang Y. Cooperative rotor-side SMES and transient control for improving the LVRT capability of grid-connected DFIG-based wind farm. IEEE Trans Appl Supercond. 2019;29(2):1–5. doi:10.1109/TASC.2018.2881315.
31. Jin C, Wang P. Enhancement of low-voltage ride-through capability for wind turbine driven DFIG with active crowbar and battery energy storage system. IEEE PES General Meeting, Minneapolis, MN, USA. 2010. p. 1–8. doi: 10.1109/PES.2010.5588180.
32. Gayathri NS, Senroy N. Wind turbine with flywheel for improved power smoothening and LVRT. 2013 IEEE Power & Energy Society General Meeting, Vancouver, BC, Canada. 2013. p. 1–5. doi: 10.1109/PESMG.2013.6672812.
33. Gayathri T, Ananth DVN, Kumar GVN, Sivanagaraju G. Enhancement in dynamic and LVRT behaviour of an EFOC controlled DFIG with integrated battery energy storage system. 2013 Annual IEEE India Conference (INDICON), Mumbai, India. 2013. p. 1–6. doi:10.1109/INDCON.2013.6726139.
34. Ibrahima KO, Zhao C. Modeling of wind energy conversion system using doubly fed induction generator equipped with battery energy storage system. 2011 4th International Conference on Electric Utility Deregulation and Restructuring and Power Technologies (DRPT), Weihai, China. 2011. p. 1780–1787. doi:10.1109/DRPT.2011.5994187.

35. Ren J, Xiao X, Zheng Z. Application of CSC-based SMES to improve the LVRT capability of DFIG-based WECS. 2020 IEEE International Conference on Applied Superconductivity and Electromagnetic Devices (ASEMD), Tianjin, China. 2020. p. 1–2. doi:10.1109/ASEMD49065.2020.9276298.
36. Okedu KE, Muyeen SM, Takahashi R, Tamura J. Comparative study between two protection schemes for DFIG-based wind generator. 2010 International Conference on Electrical Machines and Systems, Incheon, Korea (South). 2010. pp. 62–67.
37. Wang M, Xu W, Jin H, Yu X. A new control system to strengthen the LVRT capacity of DFIG based on both crowbar and DC chopper circuits. IEEE PES Innovative Smart Grid Technologies, Tianjin. 2012. p. 1–6. doi: 10.1109/ISGT-Asia.2012.6303234.
38. Pannell G, Zahawi B, Atkinson DJ, Missailidis P. Evaluation of the performance of a DC-link brake chopper as a DFIG low-voltage fault ride-through device. IEEE Trans Energy Convers. 2013;28:535–542. doi:10.1109/TEC.2013.2261301.
39. Islam MR, Ajom MG, Sheikh MRI. Application of DC chopper to augment fault ride-through of DFIG-based wind turbine. 2017 2nd International Conference on Electrical & Electronic Engineering (ICEEE), Rajshahi, Bangladesh. 2017. p. 1–4. doi:10.1109/CEEE.2017.8412918.
40. Okedu KE, Muyeen SM, Takahashi R, Tamura J. Protection schemes for DFIG considering rotor current and DC-link voltage. 2011 International Conference on Electrical Machines and Systems, Beijing, China. 2011. p. 1–6. doi:10.1109/ICEMS.2011.6073453.
41. Wu J, Zhang S, Xu D. Modeling and control of multi-terminal HVDC with offshore wind farm integration and DC chopper-based protection strategies. IECON 2013 - 39th Annual Conference of the IEEE Industrial Electronics Society, Vienna, Austria. 2013. p. 1013–1018. doi: 10.1109/IECON.2013.6699272.
42. Naderi SB, Negnevitsky M, Muttaqi KM. A modified DC chopper for limiting the fault current and controlling the DC-link voltage to enhance fault ride-through capability of doubly-fed induction-generator-based wind turbine. IEEE Trans Ind Appl. 2019;55(2):2021–2032. doi:10.1109/TIA.2018.2877400.
43. Noureldeen O, Hamdan I. Design and analysis of combined chopper–crowbar protection scheme for wind power system based on artificial intelligence. 2018 Twentieth International Middle East Power Systems Conference (MEPCON), Cairo, Egypt. 2018. p. 809–814. doi: 10.1109/MEPCON.2018.8635177.
44. Zou ZC, Mu ZL, Ou R, Lei Y, Li HB, Jiang KT. Improving dynamic performance of DFIG using rotor-side SFCL and DC-link brake chopper during grid voltage swell. 2020 IEEE International Conference on Applied Superconductivity and Electromagnetic Devices (ASEMD), Tianjin, China. 2020. p. 1–2. doi:10.1109/ASEMD49065.2020.9276126.
45. Zou ZC, Yao J. Efficient HVRT scheme of DFIG using an SSFCL–chopper considering grid voltage recovery. IEEE Trans Appl Supercond. 2021;31(8):1–3. doi:10.1109/TASC.2021.3110469.
46. Elshiekh ME, Mansour DA, Azmy AM. Improving fault ride-through capability of DFIG-based wind turbine using superconducting fault current limiter. IEEE Trans Appl Supercond. 2013;23(3):5601204. doi:10.1109/TASC.2012.2235132.
47. Moon JF, Lim SH, Kim JC, Yun SY. Assessment of the impact of SFCL on voltage sags in power distribution system. IEEE Trans Appl Supercond. 2011;21(3):2161–2164. doi:10.1109/TASC.2010.2093592.
48. Moon JF, Kim JS. Voltage sag analysis in loop power distribution system with SFCL. IEEE Trans Appl Supercond. 2013;23(3):5601504. doi:10.1109/TASC.2013.2238374.
49. Zou ZC, Xiao XY, Liu YF, Zhang Y, Wang YH. Integrated protection of DFIG-based wind turbine with a resistive-type SFCL under symmetrical and asymmetrical faults. IEEE Trans Appl Supercond. 2016;26(7):1–5. doi:10.1109/TASC.2016.2574352.
50. Zou ZC, Chen XY, Li CS, Xiao XY, Zhang Y. Conceptual design and evaluation of a resistive-type SFCL for efficient fault ride-through in a DFIG. IEEE Trans Appl Supercond. 2016;26(1):1–9. doi:10.1109/TASC.2015.2507129.

51. Chen L, Li G, Chen H, Tao Y, Tian X, Liu X, et al. Combined use of a resistive SFCL and DC-link regulation of a SMES for FRT enhancement of a DFIG wind turbine under different faults. IEEE Trans Appl Supercond. 2018;29(2):1–8. doi: 10.1109/TASC.2018.2881988
52. Du KJ, Xiao XY, Wang Y, Zheng ZX, Li CS. Enhancing fault ride-through capability of DFIG-based wind turbines using inductive SFCL with coordinated control. IEEE Trans Appl Supercond. 2019;29(2):1–6. doi:10.1109/TASC.2018.2883797.
53. Chen L, Chen H, Shu Z, Zhang G, Xia T, Ren L. Comparison of inductive and resistive SFCL to robustness improvement of a VSC-HVDC system with wind plants against DC fault. IEEE Trans Appl Supercond. 2016;26:1–8. doi:10.1109/TASC.2016.2595622.
54. Hossain M, Ali H. Asymmetric fault ride-through capability enhancement of DFIG-based variable speed wind generator by DC resistive fault current limiter. 2016 IEEE/PES Transmission and Distribution Conference and Exposition (T&D), Dallas, TX. 2016. p. 1–5. doi: 10.1109/TDC.2016.7519865.
55. Hasan J, Islam MR, Islam MR, Kouzani AZ, Mahmud MAP. A capacitive bridge-type superconducting fault current limiter to improve the transient performance of DFIG/PV/SG-based hybrid power system. IEEE Trans Appl Supercond. 2021;31(8):5603605. doi:10.1109/TASC.2021.3094422.
56. Du KJ, Ma XP, Zheng ZX, Li C, Hu W, Dong K. LVRT capability improvement of DFIG-based wind turbines with a modified bridge-resistive-type SFCL. IEEE Trans Appl Supercond. 2021;31(8):1–5. Art. no. 5603005. doi:10.1109/TASC.2021.3091114.
57. Du K, Wang Y, Zhang H. Fault ride-through capability improvement of DFIG-based wind turbine with an MBR-SFCL connected in stator side. 2020 IEEE International Conference on Applied Superconductivity and Electromagnetic Devices (ASEMD), Tianjin, China. 2020. p. 1–2. doi:10.1109/ASEMD49065.2020.9276296.
58. Chen L, Deng C, Zheng F, et al. Fault ride-through capability enhancement of DFIG-based wind turbine with a flux-coupling-type SFCL employed at different locations. IEEE Trans Appl Supercond. 2015;25(3):1–5. Art. no. 5201505. doi:10.1109/TASC.2014.2373511.
59. Islam MR, Abir DD, Islam MR, Hasan J, Huda MN, Muttaqi KM, Sutanto D. Enhancement of FRT capability of DFIG based wind farm by a hybrid superconducting fault current limiter with bias magnetic field. 2020 IEEE International Conference on Power Electronics, Smart Grid and Renewable Energy (PESGRE2020), Cochin, India. 2020. p. 1–6. doi:10.1109/PESGRE45664.2020.9070632.
60. Islam MR, Hasan J, Islam MR, Kouzani AZ, Mahmud MAP. Transient performance augmentation of DFIG based wind farms by nonlinear control of flux-coupling-type superconducting fault current limiter. IEEE Trans Appl Supercond. 2021;31(8):1–5. Art. no. 5603105. doi:10.1109/TASC.2021.3091061.
61. Islam MR, Hasan J, Islam MR, Kouzani AZ, Mahmud MAP. Optimized use of flux coupling superconducting fault current limiter to improve the performance of DFIG based wind power generation system. 2020 IEEE International Conference on Applied Superconductivity and Electromagnetic Devices (ASEMD), Tianjin, China. 2020. p. 1–2. doi:10.1109/ASEMD49065.2020.9276093.
62. Chen L, Chen H, Yang J, He H, Liu X, Yu Y, Xu Y, Wang Z, Ren L. Conceptual design and performance evaluation of a 35-kV/500-A flux-coupling-type SFCL for protection of a DFIG-based wind farm. IEEE Trans Appl Supercond. 2018;28:1–7. Art. no. 5200607. doi:10.1109/TASC.2017.2775566.
63. Chen L, Zheng F, Deng C, Li Z, Guo F. Fault ride-through capability improvement of DFIG-based wind turbine by employing a voltage-compensation-type active SFCL. Can J Electr Comput Eng. 2015;38:132–142. doi:10.1109/CJECE.2015.2406665.
64. Zheng ZX, Huang CJ, Yang RH, Xiao XY, Li CS. A low voltage ride through scheme for DFIG-based wind farm with SFCL and RSC control. IEEE Trans Appl Supercond. 2019;29(2):1–5. Art. no. 5601005. doi:10.1109/TASC.2019.2891687.

65. Ngamroo I, Karaipoom T. Cooperative control of SFCL and SMES for enhancing fault ride through capability and smoothing power fluctuation of DFIG wind farm. IEEE Trans Appl Supercond. 2014;24(5):1–4. Art. no. 5400304. doi:10.1109/TASC.2014.2340445.
66. Ou R, Xiao XY, Zou ZC, Zhang Y, Wang YH. Cooperative control of SFCL and reactive power for improving the transient voltage stability of grid-connected wind farm with DFIGs. IEEE Trans Appl Supercond. 2016;26(7):1–6. Art. no. 5402606. doi:10.1109/TASC.2016.2574344.
67. Rashid G, Ali MH. Bridge-type fault current limiter for asymmetric fault ride-through capacity enhancement of doubly fed induction machine based wind generator. 2014 IEEE Energy Conversion Congress and Exposition (ECCE), Pittsburgh, PA, USA. 2014. p. 1903–1910. doi:10.1109/ECCE.2014.6953651.
68. Rashid G, Ali MH. Transient stability enhancement of doubly fed induction machine-based wind generator by bridge-type fault current limiter. IEEE Trans Energy Convers. 2015;30(3):939–947. doi:10.1109/TEC.2015.2400220.
69. Chaudhary U, Tripathy P, Nayak SK. Application of bridge-type FCL for betterment of FRT capability for DFIG-based wind turbine. 2014 6th IEEE Power India International Conference (PIICON), Delhi, India. 2014. p. 1–6. doi:10.1109/POWERI.2014.7117687.
70. Firouzi M, Gharehpetian GB. LVRT performance enhancement of DFIG-based wind farms by capacitive bridge-type fault current limiter. IEEE Trans Sustain Energy. 2018;9(3):1118–1125. doi:10.1109/TSTE.2017.2771321.
71. Padmaja A, Shanmukh A, Mendu SS, Devarapalli R, Serrano González J, García Márquez FP. Design of capacitive bridge fault current limiter for low-voltage ride-through capacity enrichment of doubly fed induction generator-based wind farm. Sustainability. 2021;13(12):6656. doi:10.3390/su13126656.
72. Rashid G, Ali MH. Nonlinear control-based modified BFCL for LVRT capacity enhancement of DFIG-based wind farm. IEEE Trans Energy Convers. 2017;32(1):284–295. doi:10.1109/TEC.2016.2603967.
73. Rashid G, Ali MH. Asymmetrical fault ride through capacity augmentation of DFIG based wind farms by parallel resonance fault current limiter. 2016 IEEE Power and Energy Society General Meeting (PESGM), Boston, MA, USA. 2016. p. 1–5. doi:10.1109/PESGM.2016.7741506.
74. Rashid G, Ali MH. Application of parallel resonance fault current limiter for fault ride through capability augmentation of DFIG based wind farm. 2016 IEEE/PES Transmission and Distribution Conference and Exposition (T&D), Dallas, TX, USA. 2016. p. 1–5. doi:10.1109/TDC.2016.7519858.
75. Hossain MK, Ali MH. Transient stability augmentation of PV/DFIG/SG-based hybrid power system by parallel-resonance bridge fault current limiter. Electr Power Syst Res. 2016;130:89–102. doi:10.1016/j.epsr.2015.08.016.
76. Rashid G, Ali MH. Fault ride through capability improvement of DFIG based wind farm by fuzzy logic controlled parallel resonance fault current limiter. Electr Power Syst Res. 2017;146:1–8. doi:10.1016/j.epsr.2017.01.018.
77. Islam MR, Hasan J, Shipon MRR, Sadi MAH, Abuhussein A, Roy TK. Neuro fuzzy logic controlled parallel resonance type fault current limiter to improve the fault ride through capability of DFIG based wind farm. IEEE Access. 2020;8:115314–115334. doi:10.1109/ACCESS.2020.3000462.

